MIT Open Access Articles

Experimental and modeling study of the mutual oxidation of N-pentane and nitrogen dioxide at low and high temperatures in a jet stirred reactor

Massachusetts Institute of Technology

Experimental and Modeling Study of The Mutual Oxidation of N-pentane and Nitrogen Dioxide at Low and High Temperatures in a Jet Stirred Reactor

Hao Zhao*[1], Alon Grinberg Dana[2], Zunhua Zhang[1, 3], William H. Green[2], Yiguang Ju[1]

[1]Department of Mechanical and Aerospace Engineering,

Princeton University, Princeton, NJ 08544-5263, USA

[2]Department of Chemical Engineering,

Massachusetts Institute of Technology, Cambridge, MA, 02139-4307, USA

[3]School of Energy and Power Engineering,,

Wuhan University of Technology, Wuhan 430063, China

[*]Corresponding Author Email: haozhao@princeton.edu

Abstract: The mutual oxidation of n-pentane and nitrogen dioxide (NO_2) at 500-1000K has been studied at fuel lean and rich conditions (φ = 0.5 and 1.33) by using an atmospheric-pressure jet stirred reactor (JSR). N-pentane, O_2, NO, NO_2, CO, CO_2, CH_2O, C_2H_4, and CH_3CHO are simultaneously quantified, in-situ by using an electron-impact molecular beam mass spectrometer (EI-MBMS), a micro-gas chromatograph (μ-GC), and a mid-IR dual-modulation faraday rotation spectrometer (DM-FRS). At both lean and rich conditions, the experimental results show that NO_2 addition has different sensitization characteristics on n-pentane oxidation in three different temperature windows. In 550-650K, NO_2 addition inhibits low temperature oxidation. With an increase of temperature to the negative temperature coefficient (NTC) region (650-750K), NO_2 addition weakens the NTC behavior at the fuel lean condition, while the weakening effect is insignificant at the fuel rich condition. In the intermediate and high temperature region (750-1000K), high temperature

oxidation is accelerated with NO_2 addition and shifted to a lower temperature. Two kinetic models, Zhao's n-pentane/NO_x model (Zhao et al. 2019, Submitted) and a newly developed RMG n-pentane/NO_x model, were used in simulations. Both models were able to capture the temperature-dependent NO_2 sensitization characteristics successfully. According to our previous study on n-pentane/NO oxidation (Zhao et al. 2019, Submitted) and the present work, both NO and NO_2 additions have similar effects at many conditions. NO and NO_2 interconvert rapidly so the system becomes insensitive to which form of NO_x was introduced. When NO_2/NO interconversion is slow, NO_2 is relatively inert while NO can strongly promote or inhibit oxidation. In addition, NO addition delays the onset temperature of n-pentane low temperature oxidation, while NO_2 has little effect on the onset temperature. Pathway analyses and sensitivity analyses of n-pentane and NO_2 were also performed to analyze the NO_2 sensitization effects.

Key word: N-pentane, NO_2 sensitization, Low and high temperature chemistry, Jet stirred reactor

1 Introduction

Due to the increasing use of the exhaust gas recirculation (EGR) technique to reduce combustion pollutants in different types of internal engines, the effect of exhaust burned-gases (CO_2, H_2O, NO_x, etc.) on the ignition characteristics has received a lot of attention [1-5]. It is well known that trace amounts of NO_x from EGR can significantly alter the ignition kinetics at both low and high temperatures [6, 7]. The sensitization effect of NO on fuel (alkane, alcohol, aromatics, ether, etc.) oxidation has been studied in jet stirred reactors (JSR), flow reactors (FR), and homogeneous charge compression ignition (HCCI)

engines [6-13]. NO addition inhibits and promotes fuel oxidations at lower and higher temperatures, respectively. The competing reactions, $NO + HO_2 = NO_2 + OH$, $NO + RO_2 = RO + NO_2$, and $NO + OH + M = HONO + M$ mainly explain the temperature-dependent NO sensitization characteristics, where R represents the fuel radical [6, 7, 10]. Our recent paper [13] studied the NO sensitization effect on low temperature oxidation of n-pentane. It was observed that NO addition delayed the onset temperature of low temperature oxidation, suppressed the negative temperature coefficient (NTC) behavior, and shifted the high temperature oxidation to lower temperature.

However, as much as 20%-40% of the NO_x emission from diesel and gasoline engines at moderate loads is in the form of NO_2 [3, 4]; therefore, the kinetic effect of NO_2 from EGR on engine ignitions is also of importance. The NO_2 sensitization effect on oxidation of hydrogen, methane, methanol, and benzene has been investigated in FR [14-17], JSR [18, 19] and shock tube [20] at high temperatures. It was shown that NO_2 addition enhanced high temperature fuel oxidations and lowered the high temperature ignition temperature by altering the H_2/O_2 chemistry. However, to the author's knowledge, there are few kinetic studies available on the mutual oxidation of NO_2 and larger alkanes, like gasoline or diesel representatives. Especially, the effect of NO_2 addition on low temperature oxidation is not emphasized. In addition, as one of the simple alkanes with low temperature reactivity, n-pentane has been proved to be a good test fuel to study the NO_x sensitization effect on its oxidation [13, 21-23].

Motivated by the above discussion, the present paper aims to study the NO_2 sensitization effect on n-pentane oxidation at both low and high temperatures, especially to understand its impact on the onset temperature of low temperature oxidation, the transition of NTC behavior, and the high temperature ignition. The experiments of n-pentane oxidation with and without

250ppm NO_2 addition were performed at both lean and rich conditions at 500-1000K in an atmospheric-pressure JSR. The mole fractions of n-pentane, O_2, CO, CO_2, NO, NO_2, CH_2O, C_2H_4, and CH_3CHO were simultaneously quantified in-situ by using a mid-IR dual-modulation faraday rotation spectrometer (DM-FRS), an electron-impact molecular beam mass spectrometer (EI-MBMS), and a micro-gas chromatograph (μ-GC). Zhao's n-pentane/NO_x model [13] and a new n-pentane/NO_x model, developed by the open-source automated Reaction Mechanism Generation (RMG) software [24-25], were used to predict the temperature evolution of major and intermediate species and analyze the temperature-dependent NO_2 sensitization characteristics.

2 Experimental methods and kinetic models

A spherical fused silica JSR with an internal volume of 42 cm^3 was used in this study. It has four finger injectors with a 1mm inner diameter to generate intense turbulence for homogenous mixing. The JSR is covered by a stainless-steel jacket with a three-stage-regulated heating system to maintain a good thermal homogeneity throughout the reactor. The operating temperature is up to 1300K. Volumetric flow rates of gases (O_2, Ar, N_2, and NO_2) and liquid (n-pentane) were, respectively, regulated by four mass flow controllers (MKS) and a syringe pump (Harvard Apparatus, PHD 22/2000). A secondary nitrogen stream, which carried vaporized n-pentane in the pre-vaporizer to the JSR entrance, was mixed with the primary gas stream (O_2/Ar/N_2/NO_2). The temperature uniformity is within ± 3K along the vertical axis of the reactor from 500 to 1000K. Gas samples were taken by sonic probes at the exit of the JSR and analyzed by EI-MBMS, μ-GC, and DM-FRS simultaneously with cross-validation.

An EI-MBMS was employed to measure major species with a mass resolution of around 900. Gas and liquid species were calibrated directly by flowing the mixture with known mole fractions in excess N_2 and Ar. Details of the EI-MBMS and species calibrations are described elsewhere [5, 26, and 27]. Species calibrations and the electron impact ($20 \pm 1eV$) in the MBMS mainly account for the measurement uncertainty of ~10-20%. GC-TCD (Inficon 3000) was also used to quantify stable combustion species within a 5% uncertainty. The description of the μ-GC module is given elsewhere [28, 29]. A DM-FRS system, developed at Princeton, was used to measure the NO content at the outlet of the JSR within a 5% uncertainty [30, 31]. It targeted the $^{14}N^{16}O$ P(19/2)e doublet transition at 1842.946 cm^{-1} (major isotope) of NO. A laser-intensity-independent and etalon-free measurement was obtained by modulating both the applied magnetic field and the laser current. The detection limit of NO in the DM-FRS system is ~1 ppb. Further details are available elsewhere [13, 30-32].

The experiments were performed at both fuel lean and rich conditions (φ=0.5 and 1.33) with and without 250ppm NO_2 additions at 500-1000K and atmospheric pressure. Experimental conditions are shown in Table 1. The fuel concentration was fixed at 1% with varied O_2 mole fractions. The inlet volume flow rate is fixed at 969 ml/min at 295K, as such, the residence time in the reactor varies with temperature (Table 1).

Table 1 Experimental conditions

Case	Equivalence ratio	N-C_5H_{12} (%)	O_2 (%)	Ar (%)	N_2 (%)	NO_2 (ppm)	Residence time (s)	Temperature (K)
1	0.5	1	16	5	78	0	1.53-0.77	500-1000
2	0.5	1	16	5	77.975	250	1.53-0.77	500-1000
3	1.33	1	6	5	88	0	1.53-0.77	500-1000
4	1.33	1	6	5	87.975	250	1.53-0.77	500-1000

Zhao's n-pentane/NO_x model [13] and a newly developed RMG n-pentane/NO_x model were used to predict the experimental results in this paper. Zhao's model consists of an n-pentane mechanism from the AramcoMech [22] and an updated NO_x sub-mechanism from Princeton [13]. Details of Zhao's model as well as the NO_x sub-mechanism is described elsewhere [13].

The RMG model was obtained by relying on the n-pentane AramcoMech kinetic framework [22], and additional reaction subsets generated using the open-source automated Reaction Mechanism Generation software v2.1.0 [24-25]. While generating this model, particular attention was given to reactions of NO/NO_2 affecting the concentrations of oxy (RO) and peroxy (RO_2) radicals in the system. Specifically, more than eighty $RO + NO = RONO = R + NO_2$ (including $RO_2 + NO = ROONO = RO + NO_2$) reactions were automatically generated and included in the model for various radicals in the system. The reaction rates were derived from the "Radical Recombination" reaction family of RMG, and relevant thermodynamic properties of intermediates were estimated by RMG using Benson's group additivity method [33]. Another subset includes $NO_2 + RH = HONO + R$ reactions, of which more than 100 entries were generated by the "Hydrogen Abstraction" reaction family of RMG. An additional NO_x sub-mechanism was built based on the kinetic data reported in the seminal review by Dean and Bozzelli [34] with relevant updates and additions from the RMG NO_x library. In other words, both the RMG model and Zhao's model share the same n-pentane base mechanism, but have different NO_x chemistry subsets. Moreover, Zhao's model has only three $RO + NO$ pathways. The RMG model gives an improved prediction of the onset temperature of the low temperature mutual oxidation of n-pentane and NO in the experiment of [13], see Figure S1. Several reactions were modified in Zhao's model [13] from their original values (Table S1), and these modified values were kept in the RMG model. Simulations were performed in the perfectly stirred reactor module of Chemkin software [35].
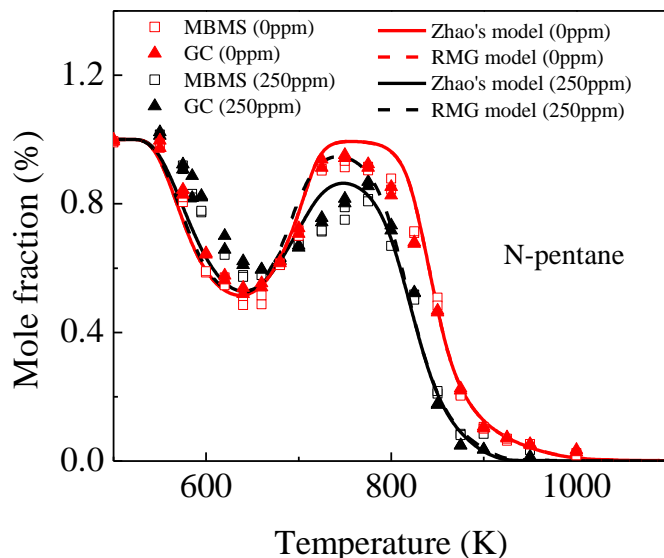
3 Results and discussion

Fig. 1 Temperature evolution of the mole fraction of n-pentane at the fuel lean conditions ($\varphi=0.5$) with and without 250ppm NO_2 addition in a JSR, conditions of Table 1.

The temperature evolution of n-pentane mole fraction at the fuel lean conditions ($\varphi=0.5$) with and without 250ppm NO_2 addition is shown in Figure 1. The low temperature oxidation of n-pentane is clearly observed in the experiment. EI-MBMS and μ-GC measurements agree within 10%. Both Zhao's model and the RMG model predict the temperature evolution of n-pentane oxidation without NO_2 addition reasonably well as expected since they are both based on the n-pentane model of [22] which was adjusted to match JSR data on n-pentane. With 250ppm NO_2 addition, it is seen that NO_2 sensitizes the oxidation significantly. Firstly, NO_2 slows down low temperature oxidation in 550-650K, but does not change the onset temperature of low temperature oxidation. Secondly, NO_2 suppresses the NTC behavior in the NTC region (650-750K). Furthermore, NO_2 shifts high temperature oxidation to lower temperature in the intermediate and high temperature region (750-1000K).
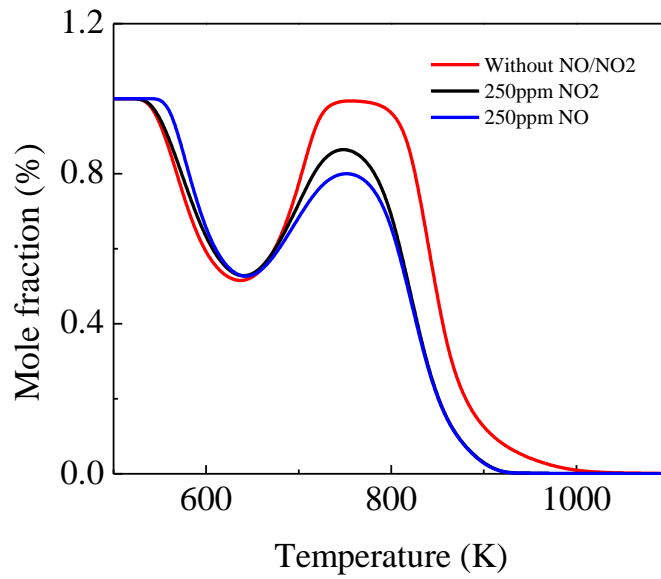
Fig. 2 Temperature evolution of the mole fraction of n-pentane at the fuel lean conditions (φ=0.5) with 250ppm NO_2, with 250ppm NO, and without NO_2/NO additions using Zhao's model.
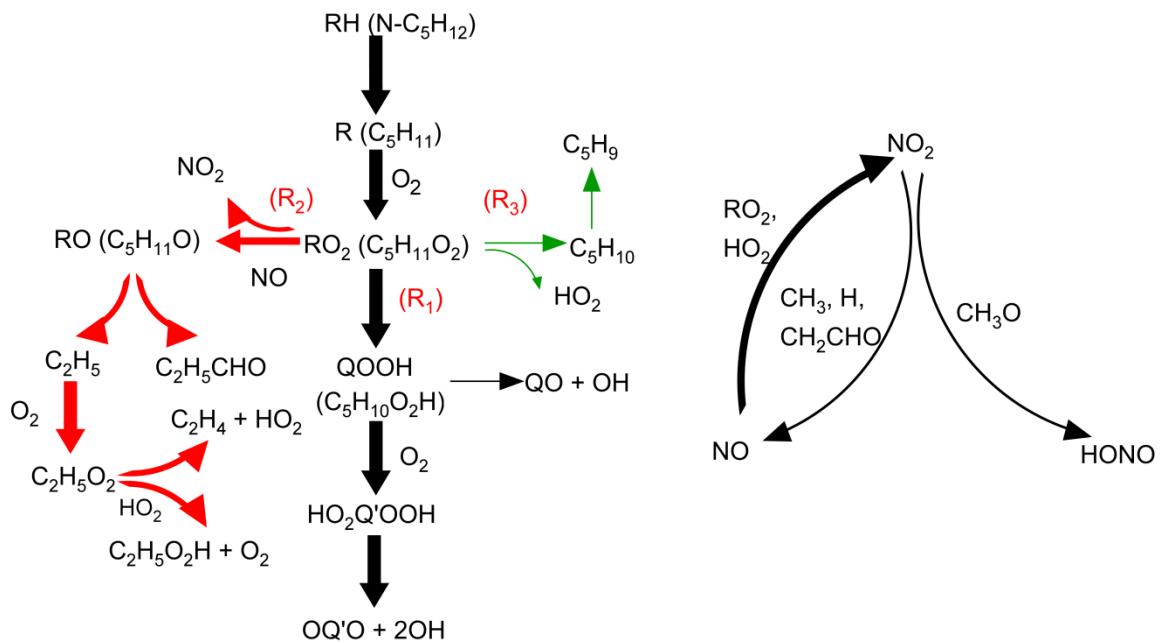

Fig. 3 Pathway analysis of n-pentane and NO_2 at 600K for a JSR in the fuel lean condition (φ=0.5) with 250ppm NO_2 addition using the RMG model

The NO sensitization effect on n-pentane oxidation has been investigated in our last study [13]. In this paper, the n-pentane oxidation at fuel lean conditions with the same doping concentration of NO and NO_2 are compared to simulations in Figure 2. It is seen that both NO and NO_2 additions show the three similar sensitization characteristics in low and intermediate temperatures. However, when the normal oxidation chain branching is suppressed, NO_2 addition has less effect on fuel oxidation. In addition, NO addition delays the onset temperature of n-pentane low temperature oxidation, while NO_2 has little effect on the onset temperature.

To explain the impact of NO_2 addition on n-pentane oxidation at low and high temperatures, pathway analyses of n-pentane and NO_2 were respectively performed at 600, 700, and 800K by using the RMG model at the lean condition with 250ppm NO_2 addition (Figures 3-5). The pathway analysis of n-pentane in Figure 3 shows that there are three reaction channels of RO_2 consumption,

$$RO_2 = QOOH \tag{R_1}$$

$$RO_2 + NO = RO + NO_2 \tag{R_2}$$

$$RO_2 + M = C_5H_{10} + HO_2 + M \tag{R_3}$$

Reaction R_1 is part of the typical low temperature oxidation channel, which proceeds through competing reactions between QOOH decomposition and $QOOH + O_2$. Reaction R_2 describes RO_2 consumption by NO, and reaction R_3 is a decomposition channel forming HO_2. Since RO and HO_2 (produced in reaction channels R_2 and R_3) are much less reactive than OH radicals (produced from QOOH subsequent reaction R_1) at low temperature, reaction channels R_2 and R_3 (Figure 3, red and green pathways) play inhibiting roles in n-pentane oxidation in 550-650K. As for NO_2-related pathways, it is noted that NO and HONO are produced from NO_2, respectively, mainly through reactions R_4-R_7,

$$NO_2 + CH_3 = CH_3O + NO \tag{R_4}$$

$$NO_2 + H = OH + NO \tag{R_5}$$

$$NO_2 + CH_2CHO = CH_2O + HCO + NO \tag{R_6}$$

$$NO_2 + CH_3O = HONO + CH_2O \tag{R_7}$$

while at low temperature, NO reacts with RO_2 and HO_2 to regenerate NO_2 quickly through reactions R_2 and R_8, respectively.

$$HO_2 + NO = OH + NO_2 \tag{R_8}$$

Therefore, according to the pathway analysis, NO and HONO are a quasi-steady-state (QSS) species and a stable species at low temperature, respectively, and the rates of interconversion among NO, NO_2, and HONO are quantified below in terms of reaction characteristic time scales (Fig. 11). Reaction channel R_1 (Figure 3, black pathway) promotes low temperature oxidation of n-pentane through the formation of QOOH, O_2QOOH, and subsequent two OH radicals. However, with 250ppm NO_2 addition, NO is produced from NO_2 mainly through reactions R_4-R_6, and then immediately consumes RO_2 and HO_2 through the inhibiting reaction channel R_2 and R_3 (Figure 3, red and green pathways), competing with R_1 (Figure 3, black pathway). Therefore, the reactivity slows down.
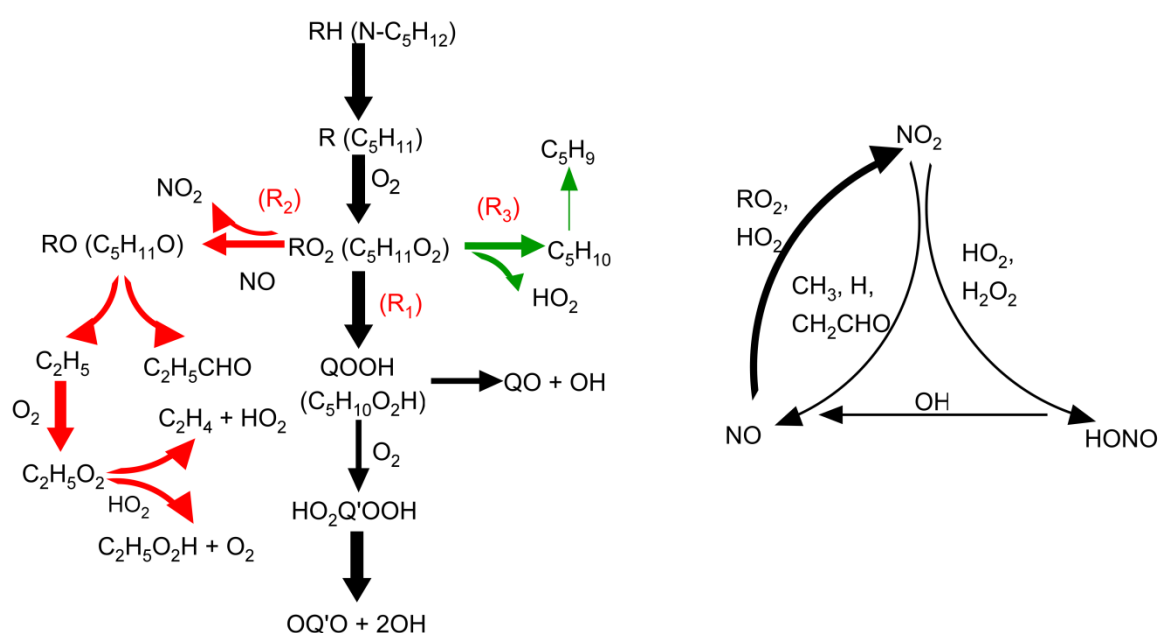
Fig. 4 Pathway analysis of n-pentane and NO_2 at 700K for a JSR in the fuel lean condition ($\varphi=0.5$) with 250ppm NO_2 addition using the RMG model

In the NTC region in Figure 4, the pathway analysis of NO_2 shows that HONO, produced from reaction R_9 and R_{10}, begins to decompose to NO through R_{11},

$$NO_2 + HO_2 = HONO + O_2 \tag{R_9}$$

$$NO_2 + H_2O_2 = HONO + HO_2 \tag{R_{10}}$$

$$HONO + M = OH + NO + M \tag{R_{11}}$$

and NO is still a QSS species, which is also clarified in terms of reaction characteristic time scales in Figure 11. The combination of R_9 and R_{11} converts a relatively inactive radical, HO_2, into a very active OH radical, and the additional NO generated by R_{11} does the same thing via R_8. This also reduces radical loss via $HO_2 + HO_2$, which is very important in NTC [36]. Hence, reactivity increases, and NO_2 addition partially suppresses NTC behavior.
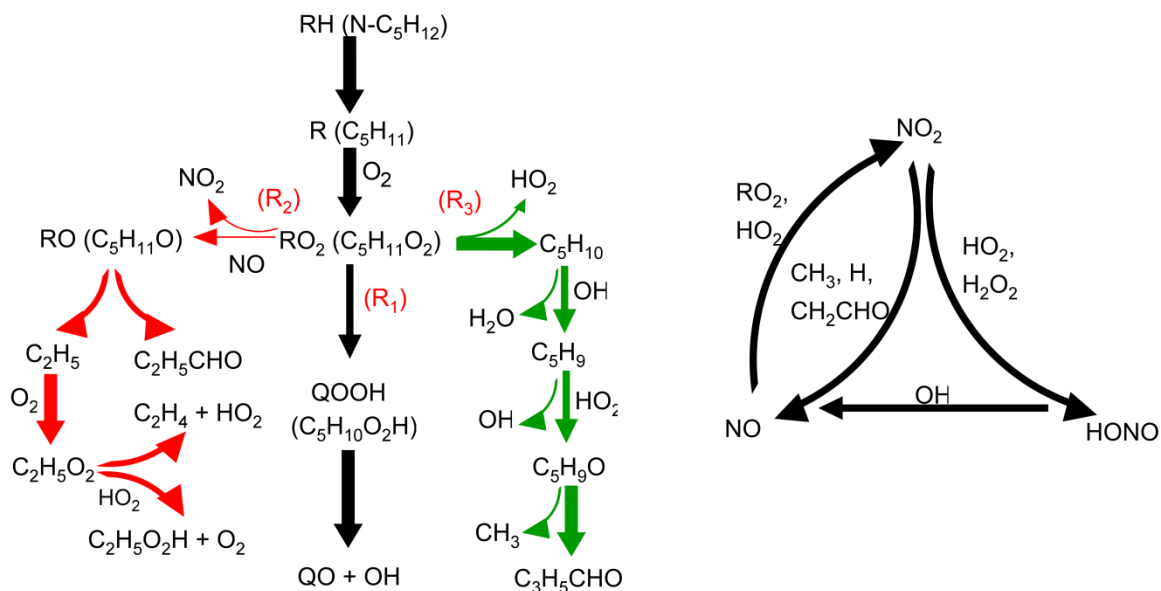

Fig. 5 Pathway analysis of n-pentane and NO_2 at 800K in the fuel lean condition ($\varphi=0.5$) with 250ppm NO_2 addition using the RMG model

With an increase of temperature to 800K in Figure 5, reaction channel R_3 (Figure 5, green pathway) plays a dominant role of the RO_2 consumption in the pathway analysis of n-pentane. A significant dissociation of HONO into OH and NO through reaction R_{11} in the pathway analysis of NO_2 also occurs. Without NO_2, reaction channel R_3 (Figure 5, green pathway) suppresses the oxidation as HO_2 is relatively stable. However, when NO_2 is added, two OH radicals are overall formed from two HO_2 radicals through the reaction series R_8-R_{11} in reaction channel R_3, promoting the oxidation. In addition, CH_3, produced in the pathway of reaction channel R_3 (Figure 5, green pathway), forms H and OH radicals through this series of reactions.

$$NO_2 + CH_3 = CH_3O + NO \tag{R_4}$$

$$CH_3O + M = CH_2O + H + M \tag{R_{12}}$$

$$CH_2O + NO_2 = HCO + HONO \tag{R_{13}}$$

$$HONO + M = OH + NO + M \tag{R_{11}}$$

This also contributes to the promoting effect of NO_2 in the intermediate and high temperature region.

Based on the discussion above, the NO_x effect on alkene oxidation may be interpreted as following.

(a) When the oxidation is running at the temperatures with enough HO_2 and OH radicals, NO_x behaves as a catalyst, and the catalytic cycle time $NO_2 \rightarrow NO \rightarrow NO_2$ is relatively short compared to the residence time in the reactor.

(b) At conditions where the normal oxidation chain branching is suppressed, the NO_x interconversion is slow enough that the system is sensitive to which species, NO or NO_2, is introduced. NO_2 addition has less effect on the oxidation at these conditions than NO because R_2 and R_8 are always fast but some of the NO_2 reactions are slow.
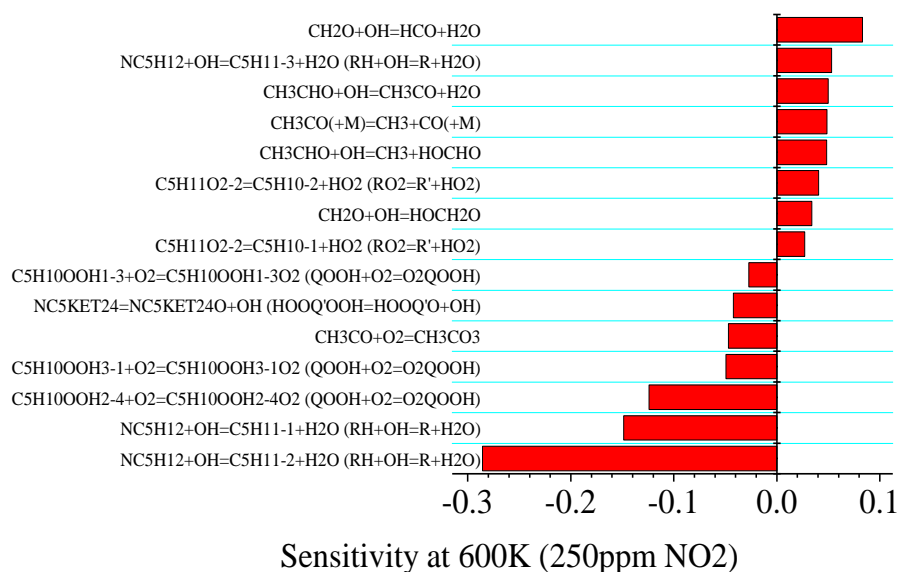
Fig. 6 Sensitivity analysis of n-pentane in the fuel lean condition (φ=0.5) with 250ppm NO_2 addition using the RMG model in a JSR at 600K, conditions of Table 1.

To cross-validate the pathway analyses, the sensitivity analyses of the n-pentane mole fraction at the fuel lean condition with 250ppm NO_2 addition were also performed at 600, 700, and 800K, respectively, by using the RMG model (Figures 6-8). It can be seen from Figure 6 that the H abstraction reactions of n-pentane, HOOQ'OOH decomposition reaction, QOOH addition reaction with O_2, and the RO_2 decomposition reactions are the most sensitive reactions at 600K. It is known that the H abstraction reactions of fuels generally rank high in the sensitivity analysis. The latter two sets of reactions belong to the reaction channels R_1 and R_3 of RO_2 consumption. At 700K, the sensitivity analysis in Figure 7 shows that the most sensitive reactions are the H abstraction reactions of n-pentane, reactions through the three RO_2 consumption channels R_1-R_3, and NO_2/NO conversion reactions (R_8 and R_{12}). Therefore, in the NTC region, all of the three reaction channels of RO_2 consumption are of importance and affect n-pentane oxidation. With an increase of temperature to 800K, the H abstraction reactions of n-pentane by HO_2 and OH, the decomposition of RO_2 to make HO_2 through R_3, NO_2/NO conversion reactions (R_8, R_9, and R_{11}), and reactions of HO_2/H_2O_2 chemistry are the

13

most sensitive reactions. At this temperature, chain branching mainly occurs via reactions involving HO_2/H_2O_2 through R_9 and R_{10} rather than the QOOH cycle which is dominant at lower T. It is noted that only reaction channel R_3 is the main RO_2 consumption pathway in the sensitivity analysis at 800K, which is in agreement with the pathway analysis at 800K (Figure 5).
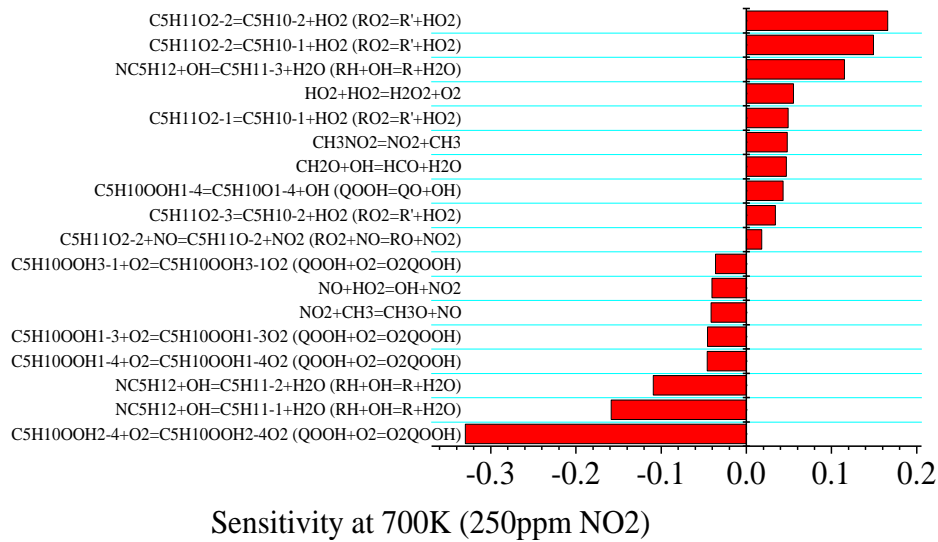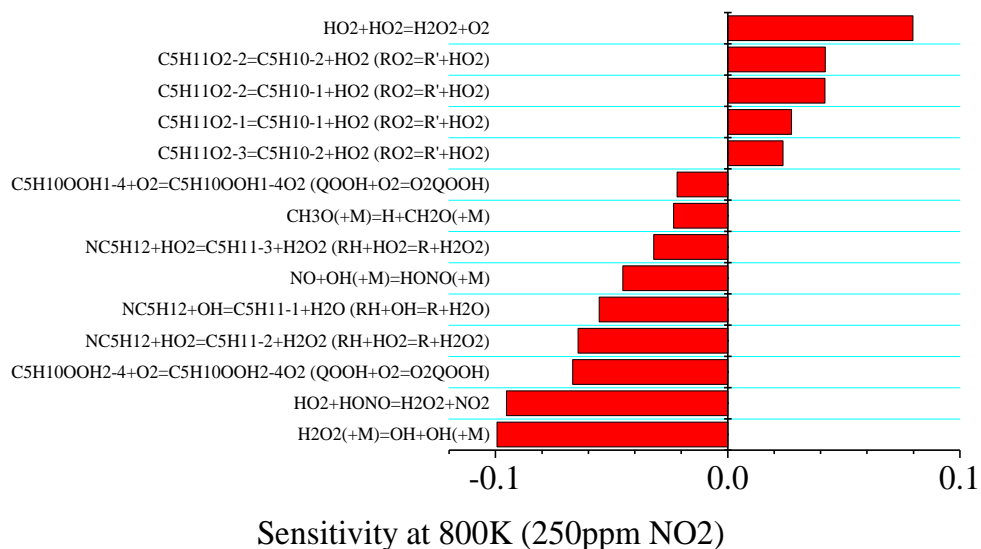

Fig. 7 Sensitivity analysis of n-pentane at 700K in the fuel lean condition (φ=0.5) with 250ppm NO_2 addition using the RMG model in a JSR, conditions of Table 1.

Fig. 8 Sensitivity analysis of n-pentane at 800K in the fuel lean condition (φ=0.5) with 250ppm NO_2 addition using the RMG model in a JSR, conditions of Table 1.
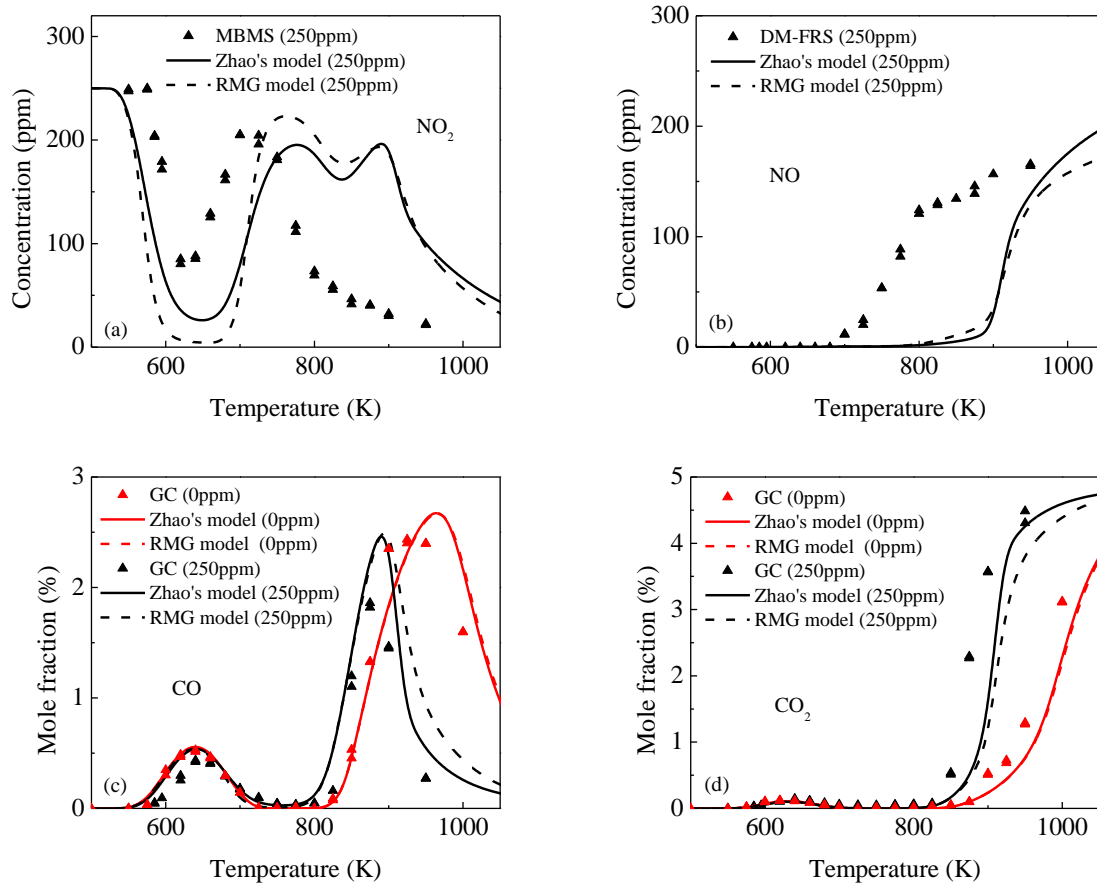
Fig. 9 Temperature evolutions of the concentrations of NO_2, NO, CO, and CO_2 at the fuel lean conditions ($\varphi=0.5$) with and without 250ppm NO_2 addition in a JSR, conditions of Table 1.

Figure 9 (a)-(d) shows the temperature evolutions of NO_2, NO, CO, and CO_2 at fuel lean condition ($\varphi=0.5$), respectively. Generally, both Zhao's model and the RMG model have captured the major species temperature evolutions well. However, the models predictions of the NO and NO_2 evolution curves at intermediate and high temperatures are shifted to higher temperatures. This might be related to uncertainties in pathways of RO_2+NO and NO_2/NO interconversion reactions. It is noted that the temperature evolutions of NO_2 and NO in Figure 9 (a) and (b) correspond to the pathway analyses of NO_2 at 600, 700, and 800K. According to the RMG model, the major nitrogen-related species in the oxidation are NO,

NO_2, and HONO. The pathway analysis of NO_2 at 600K (Figure 3) shows that HONO is accumulated through reaction R_7, while NO is a quasi-steady-state species. This explains why the NO_2 concentration dramatically decreases with temperature and NO is experimentally unobservable at 550-650K in Figure 9 (a) and (b), respectively. With an increase of temperature to the NTC region, HONO begins to decompose to NO through reaction R_{11}. Thus, NO_2 concentration recovers at 650-750K in the experiment. Above 750K, as CH_3 and HO_2 concentrations dramatically increase with temperature, NO_2 consumption through reactions R_4, R_9, and R_{10} increases accordingly. Meanwhile, HONO decomposition rate (reaction R_{11}) also increases significantly with temperature. Therefore, the NO_2 concentration decreases while NO begins to accumulate with temperature.

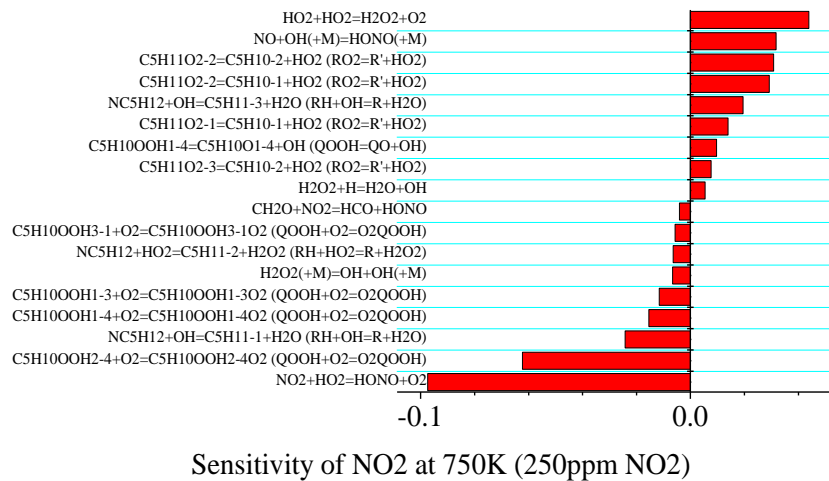Sensitivity of NO2 at 750K (250ppm NO2)

Fig. 10 Sensitivity analysis of NO_2 at 750K in the fuel lean condition (φ=0.5) with 250ppm NO_2 addition using the RMG model in a JSR, conditions of Table 1.

To clarify the model prediction uncertainty of NO_2 at intermediate temperatures (700-800K), the sensitivity analysis of the NO_2 mole fraction at the fuel lean condition with 250ppm NO_2 addition was also performed at 750K by using the RMG model (Figures 10). It is seen that the H abstraction reactions of n-pentane, QOOH addition reaction with O_2, the RO_2 decomposition reactions, reactions of HO_2/H_2O_2 chemistry, and NO_2/HONO/NO conversion

reactions (R_9, R_{11}, and R_{13}) are the most sensitive reactions at this temperature range. Therefore, the main uncertainty may come from the NO_x sub-model, especially involving in HONO chemistry. Quantification of HONO is necessary to verify the model uncertainty in predicting nitrogen-containing species in the future study.

Furthermore, characteristic time scales of NO, NO_2, and HONO interconversion reactions are compared at different temperatures at the fuel lean condition with 250ppm NO_2 addition using The RMG model in Figure 11. According to the discussion above, NO mainly forms NO_2 through reactions R_2 and R_8; NO_2 forms NO through R_4-R_6; NO_2 forms HONO through R_7, R_9, and R_{10}; and HONO mainly produces NO through R_{11}. The characteristic time scale of NO_x interconversion is defined as

$$\tau_{j_1 \to j_2} = \frac{[C_{j_1}]}{\sum_{i=1}^{n} r_{i, j_1 \to j_2}} , \text{j} = \{\text{NO, NO}_2\text{, HONO}\}$$

where, $\tau_{j_1 \to j_2}$ is the characteristic time scale of j_1 to j_2, $[C_{j_1}]$ is the volume concentration of C_{j_1}, and $r_{i, j_1 \to j_2}$ is the ith reaction rate of j_1 to j_2 evaluated at steady state in JSR. At the low temperature and NTC regions (550-750K), Conversion of NO to NO_2 is much faster than the other three characteristic time scales, and HONO decomposition is very slow. Therefore, NO is likely a QSS species and HONO is a stable molecule, which is in agreement with the NO_2 pathway analysis in Figure 3 and NO and NO_2 mole fraction profiles in Figure 9. Above 800K, the conversion of NO_2 to NO becomes comparable with the time scale of NO to NO_2, and even faster at higher temperatures. In other words, the interconversion of NO and NO_2 is very fast at this temperature range, and there is a significant dissociation of HONO to NO as well. NO, NO_2, and HONO reach steady state quickly within the residence time in the JSR, which agrees with the pathway analysis of NO_2 in Figure 5, and explains the similar sensitized effects of NO and NO_2 at intermediate and high temperatures in Figure 2. Moreover, above 900K, the time scale of NO_2 to NO is faster than that of NO to NO_2. It

explains why the NO_2 concentration decreases while NO begins to accumulate with temperature in this region. In addition, $\tau_{NO \rightarrow NO_2}$ and $\tau_{NO_2 \rightarrow HONO}$ increase at higher temperature due to a decrease in $[HO_2]$ at these conditions.
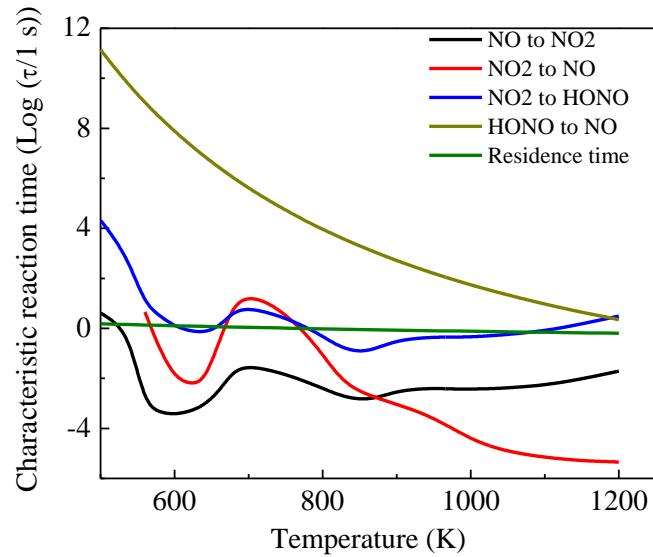

Fig. 11 Temperature evolutions of characteristic time scales of NO, NO_2, and HONO interconversion reactions at the fuel lean conditions (φ=0.5) with 250ppm NO_2 addition using the RMG model in a JSR, conditions of Table 1.
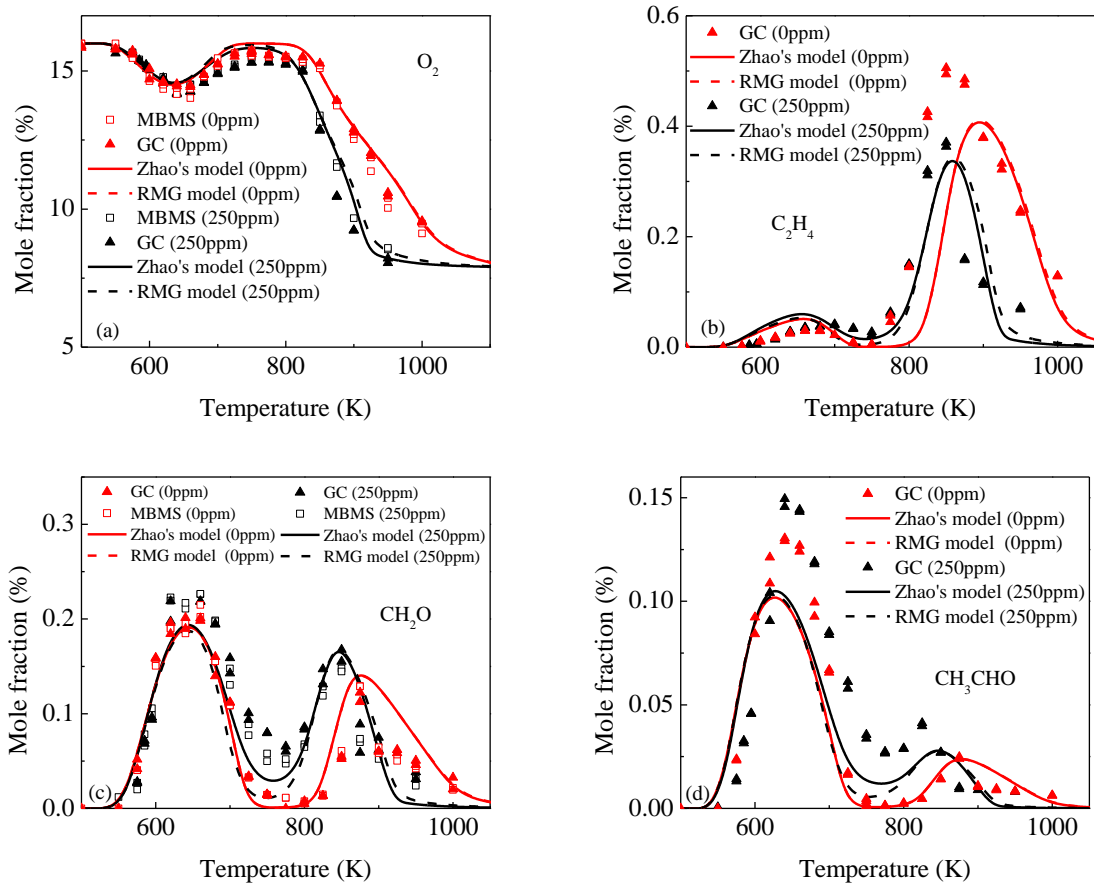
Fig. 12 Temperature evolutions of the mole fractions of O_2, C_2H_4, CH_2O, and CH_3CHO at the fuel lean conditions ($\varphi=0.5$) with and without 250ppm NO_2 addition in a JSR, conditions of Table 1.

The temperature evolutions of O_2, C_2H_4, CH_2O, and CH_3CHO are shown in Figure 12 (a)-(d), respectively. It is seen that both models predict O_2, C_2H_4, CH_2O, and CH_3CHO mole fraction profiles at low and high temperatures very well, indicating good model performances in capturing the pathways of the major intermediates.
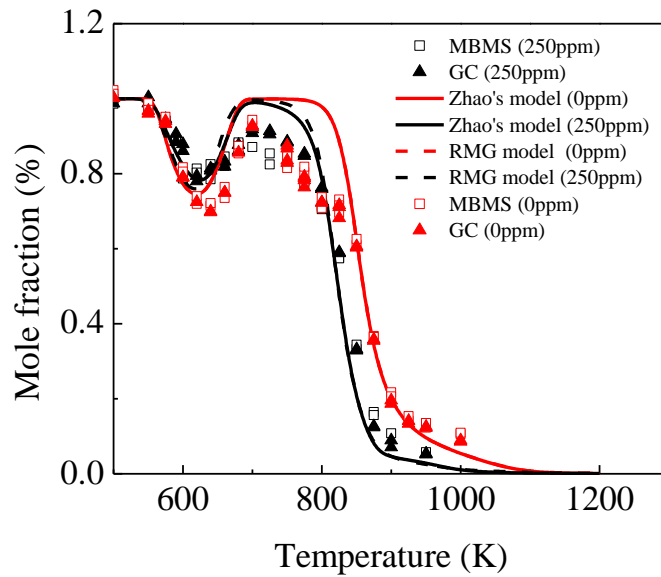
Fig. 13 Temperature evolution of the mole fraction of N-pentane at the fuel rich conditions (φ=1.33) with and without 250ppm NO_2 addition in a JSR, conditions of Table 1.

Figure 13 depicts the mole fraction of n-pentane versus the gas temperature at the fuel rich conditions (φ=1.33) with and without 250ppm NO_2 addition. It is seen that the low temperature oxidation window of n-pentane at the fuel rich condition is much smaller than that at the lean condition in Figure 1. According to the sensitivity analysis of n-pentane, RH + OH is the most sensitive H abstraction reaction of n-pentane at low temperature. However, in the fuel rich condition, O_2 mole fraction is reduced, and reactions involving O_2, like RH + O_2, R + O_2 and QOOH + O_2, are suppressed. Therefore, the low temperature oxidation is suppressed at the lower oxygen mole fraction condition. In addition, NO_2 does not have a significant weakening effect on the NTC behavior, as reaction channel R_2 is also suppressed at the condition with lower O_2 mole fraction.
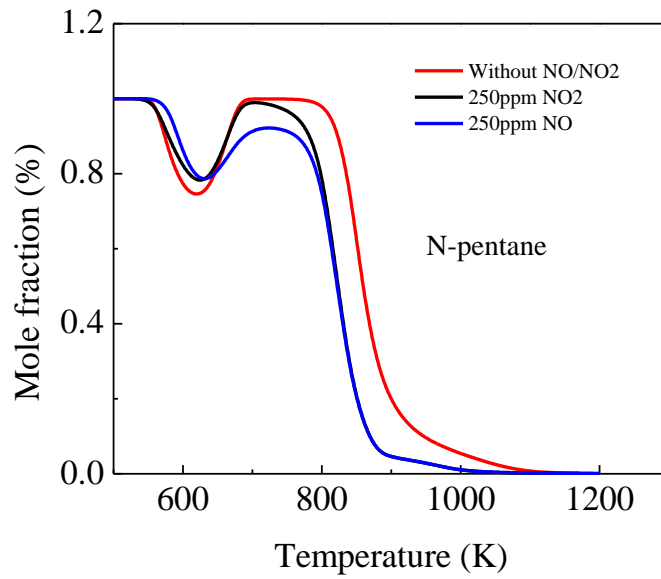
Fig. 14 Temperature evolution of the mole fraction of n-pentane in the fuel rich conditions ($\varphi=1.33$) with 250ppm NO_2, with 250ppm NO, and without NO_2/NO additions using Zhao's model.

Furthermore, the n-pentane oxidations at the fuel rich conditions with the same doping concentration of NO and NO_2 are compared in Figure 14. Similar to the fuel lean conditions, it is seen that NO_2 addition has little effect on the onset temperature, and has less suppressive effect on the NTC behavior than NO addition at the fuel rich condition.
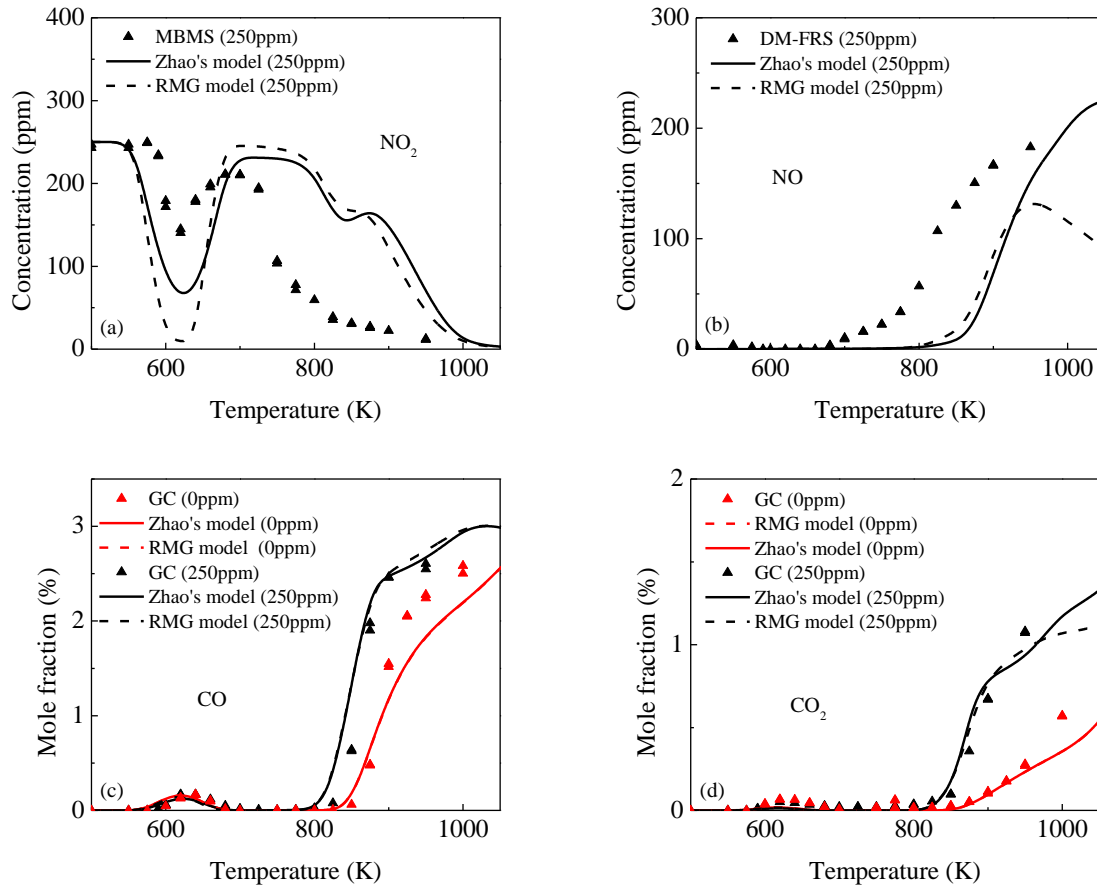
Fig. 15 Temperature evolutions of the concentrations of NO_2, NO, CO, and CO_2 at the fuel rich conditions (φ=1.33) with and without 250ppm NO_2 addition in a JSR, conditions of Table 1.

Figure 15 (a)-(d) and Figure 16 (a)-(d) depict mole fractions of NO_2, NO, CO, CO_2, O_2, C_2H_4, CH_2O, and CH_3CHO versus the gas temperature at the fuel rich conditions (φ=1.33) with and without NO_2 additions, respectively. Both models predict the mole fractions of major intermediates and products well at low and high temperatures. However, the models still show prediction delays of the NO and NO_2 evolution curves at intermediate and high temperatures. Especially, above 925K, unlike the experimental result and Zhao's model prediction, the predicted NO mole fraction decreases with temperature in the RMG model.

NO sensitivities analysis using the RMG model (Figure 17) shows that the uncertainty may come from reactions of HCCO + NO = CO + HCNO and HCCO + NO = CO_2 + HCN.
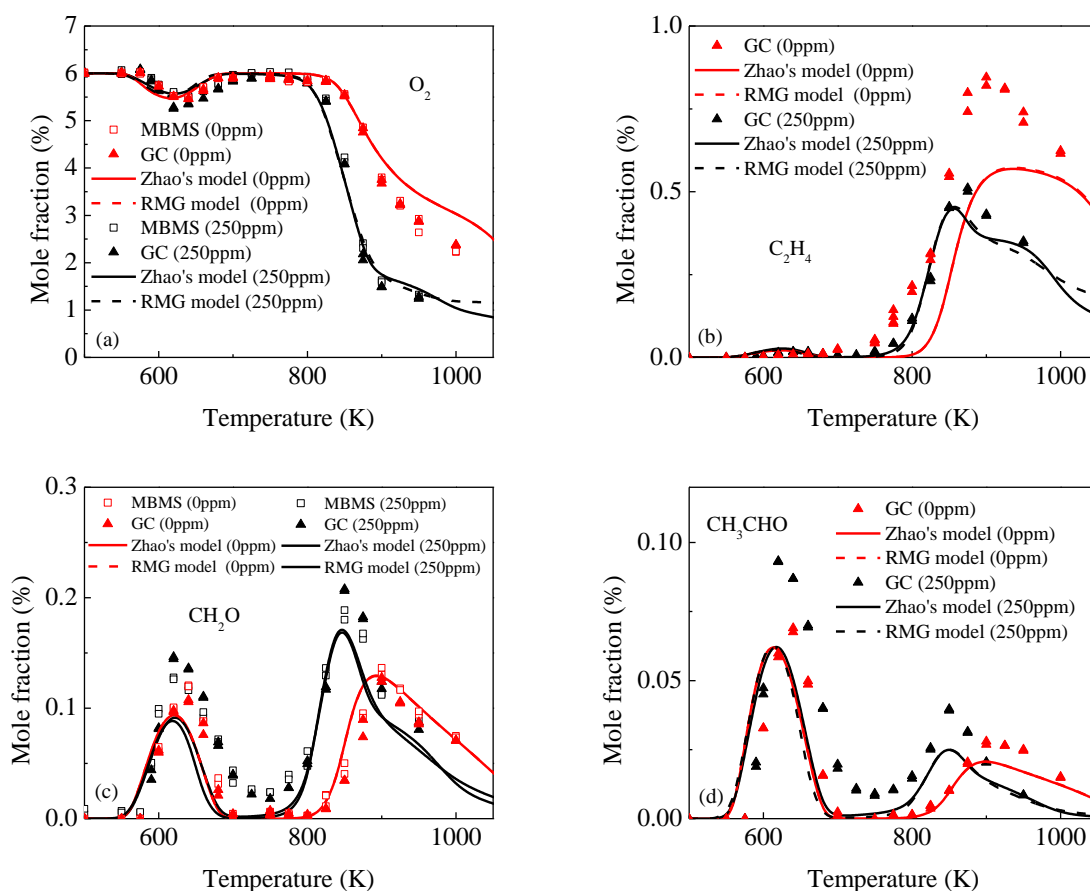

Fig. 16 Temperature evolutions of the concentrations of O_2, C_2H_4, CH_2O, and CH_3CHO at the fuel rich conditions (φ=1.33) with and without 250ppm NO_2 addition in a JSR, conditions of Table 1.
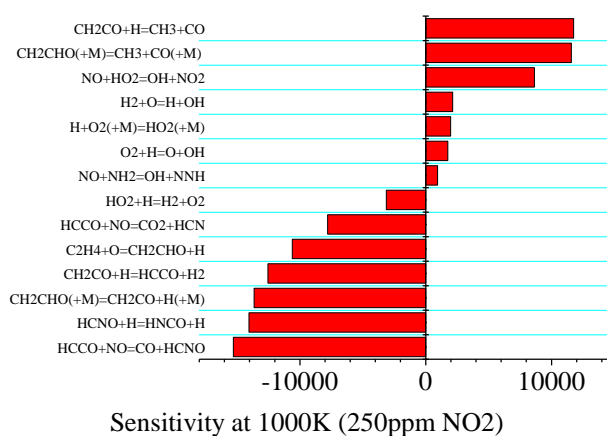

Sensitivity at 1000K (250ppm NO2)

Fig. 17 Sensitivity analysis of NO at 1000K in the fuel rich condition (φ=1.33) with 250ppm NO$_2$ addition using the RMG model in a JSR, conditions of Table 1.

4 Conclusions

The mutual oxidation of n-pentane and NO$_2$ was studied at fuel lean and rich (φ=0.5 and 1.33) conditions with and without 250ppm NO$_2$ additions at 500-1000K. Experimental results show that at the conditions studied, NO$_2$ addition modestly slows oxidation below 700 K, but accelerates it at higher temperatures. First, NO$_2$ slows down low temperature oxidation in 550-650K. Second, NO$_2$ accelerates oxidation, i.e., suppresses the NTC behavior, in the NTC region (650-750K). Furthermore, NO$_2$ shifts high temperature oxidation to lower temperature in the intermediate and high temperature region (750-1000K). Two kinetic models, Zhao's model and a new developed RMG model, were used to predict experimental results. Based on our previous study on the mutual oxidation of n-pentane and NO [13] and the present work, it is seen that both NO and NO$_2$ additions show similar sensitization characteristics in low and intermediate temperatures. However, when the n-pentane chemistry is suppressed, NO$_2$ addition has less effect on the oxidation. In addition, NO addition delays the onset temperature of n-pentane low temperature oxidation, while NO$_2$ has little effect on the onset temperature.

Pathway analyses reveal that reactions R$_1$-R$_3$ are the dominant RO$_2$ consumption channels. With NO$_2$ addition, at 550-650K, reaction channel R$_2$ inhibits n-pentane oxidation where the NO is primarily formed by R$_4$ and R$_5$. Nevertheless, at 650-750K, reaction channel R$_2$ plays a promoting role in accelerating n-pentane oxidation and suppressing the NTC behavior through R$_8$-R$_{11}$. In the intermediate and high temperature regions, NO$_2$ addition significantly promotes high temperature oxidation through reaction channel R$_3$ followed byR$_4$ and R$_8$-R$_{13}$, and shifts it to lower temperature. Both Zhao's model and RMG model predict the

experimental results reasonably well at both fuel rich and lean conditions, except for prediction delays of the NO and NO_2 evolution curves. It is suggested that the NO/NO_2 interconversion reactions are mispredicted at 700-900 K, perhaps because additional fuel/NO_x reaction pathways are needed, or the estimated Ea's for some of the reactions involving HONO are inaccurate.

In summary, the NO_x effect on alkenes oxidation is interpreted as the following steps.

(a) When the oxidation is running at the temperatures with enough HO_2 and OH radicals, NO_x behaves as a catalyst, and the catalytic cycle time $NO_2 \rightarrow NO \rightarrow NO_2$ is relatively short compared to the residence time in the reactor.

(b) At conditions where the normal oxidation chain branching is suppressed, the NO_x interconversion is slow enough that the system is sensitive to which species, NO or NO_2, is introduced. NO_2 addition has less effect on the oxidation at these conditions than NO because R_2 and R_8 are always fast but some of the NO_2 reactions are slow.

6 References

[1] J. E. Dec, Advanced compression-ignition engines—understanding the in-cylinder processes, Proc. Combust. Inst. 32 (2009) 2727−2742.

[2] V. Knop, S. Jay, Latest Developments in Gasoline Auto-Ignition Modelling Applied to an Optical CAI (Tm) Engine, Oil Gas Sci. Technol. Rev. IFP, 61 (2006), pp. 121-137

[3] J.C. Hilliard, R.W. Wheeler, Nitrogen Dioxide in Engine Exhaust, SAE Technical Paper 790691, 1979

[4] M Lenner, Nitrogen dioxide in exhaust emissions from motor vehicles, Atmos. Environ. (1967) Volume 21, Issue 1, 1987, Pages 37-43

[5] H. Zhao, X. Yang, Y, Ju, Kinetic studies of ozone assisted low temperature oxidation of dimethyl ether in a flow reactor using molecular-beam mass spectrometry, Combust. Flame, 173 (2016) 187-194.

[6] G. Moréac, P. Dagaut, J.F. Roesler, M. Cathonnet, Nitric oxide interactions with hydrocarbon oxidation in a jet-stirred reactor at 10 atm, Proc. Combust. Inst. 2 (2002) 240–251.

[7] P.A. Glaude, N. Marinov, Y. Koshiishi, et al., Kinetic modeling of the mutual oxidation of no and larger alkanes at low temperature, Energy Fuels 19 (2005) 1839-1849

[8] P. Dagaut, A. Nicolle, Experimental study and detailed kinetic modeling of the effect of exhaust gas on fuel combustion: mutual sensitization of the oxidation of nitric oxide and methane over extended temperature and pressure ranges, Combust. Flame, 140 (2005), pp. 161-171.

[9] P. Dagaut, J. Luche, et al, The low temperature oxidation of DME and mutual sensitization of the oxidation of DME and nitric oxide: Experimental and detailed kinetic modeling, Combust. Sci. Tech, 165 (2001) 61-84

[10] T. Faravell, A. Frassoldati, E. Ranzi, Combust. Flame 132 (2003) 188-207

[11] F. Contino, F. Foucher, P. Dagaut, et al, Experimental and numerical analysis of nitric oxide effect on the ignition of iso-octane in a single cylinder HCCI engine, Combust. Flame 160 (2013) 1476−1483.

[12] J.C.G. Andrae, Kinetic modeling of the influence of NO on the combustion phasing of gasoline surrogate fuels in an HCCI engine, energy Fuels, 27 (2013) 7098-7107

[13] Hao Zhao, Lingnan Wu, Charles Patrick, et al, Kinetic study of Low Temperature Oxidation of N-pentane with Nitric Oxide Addition in a Jet Stirred Reactor, Proc. Combust. Inst. (2019), Submitted.

[14] A.A. Konnov, J.N. Zhu, J.H. Bromly, D. Zhang, The effect of NO and NO_2 on the partial oxidation of methane: experiments and modeling, Proc. Combust. Inst. 30 (2005) 1093-1100

[15] T. Am Ano, F.L. Dryer, Effect of dimethyl ether, NOx, and ethane on CH4 oxidation: High pressure, intermediate-temperature experiments and modeling, Proc. Combust. Inst. 27 (1998) 397-404

[16] Y.L. Chan, F.J. Barnes, J.H. Bromly, A.A. Konnov, D.K. Zhang, The differentiated effect of NO and NO2 in promoting methane oxidation, Proc. Combust. Inst. 33 (2011) 441-447

[17] A.B. Lovell, K. Brezinsky, I. Glassman, Benzene oxidation perturbed by NO2 addition, Proc. Combust. Inst. 22 (1989) 1063-1074

[18] G. Dayma, P. Dagaut, Effects of air contamination on the combustion of hydrogen – effect of NO and NO_2 addition on hydrogen ignition and oxidation kinetics, Combust. Sci. Technol. 178 (2006) 1999-2024

[19] G. Dayma, K.H. Ali, P Dagaut, Experimental and detailed kinetic modeling study of the high pressure oxidation of methanol sensitized by nitric oxide and nitrogen dioxide, Proc. Combust. Inst. 31 (2007) 411-418

[20] M.W. Slack, A.R. Grillo Combust. Flame, 40 (1981), pp. 155-172

[21] J. Bugler, K.P. Somers, E.J. Silke, H.J. Curran, Revisiting the kinetics and thermodynamics of the low-temperature oxidation pathways of alkanes: a case study of the three pentane isomers, J. Phys. Chem. A, 119 (2015), pp. 7510-7527

[22] J. Bugler, A. Rodriguez, et al, An experimental and modeling study of n-pentane oxidation in two jet-stirred reactors: The importance of pressure-dependent kinetics and new reaction pathways, Proc. Combust. Inst. 36 (2017) 441-448

[23] A. Rodriguez, O. Herbinet, et al, Measuring hydroperoxide chain-branching agents during *n*-pentane low-temperature oxidation, Proc. Combust. Inst. 36 (2017) 333-342

[24] C.W. Gao, J.W. Allen, W.H. Green, R.H. West, Reaction Mechanism Generator: Automatic construction of chemical kinetic mechanisms, Comput. Phys. Commun. 203 (2016) 212-225.

[25] A.G. Dana, B. Buesser, S.S. Merchant, W.H. Green, Int. J. Chem. Kinet. (2018) 1-16.

[26] D. Felsmann, H. Zhao, Q. Wang, et al., Contributions to improving small ester combustion chemistry: Theory, model and experiments, Proc. Combust. Inst. 36 (2017) 543-551.

[27] L. Tran, J. Pieper, H. Carstensen, H. Zhao, et al., Experimental and kinetic modeling study of diethyl ether flames, Proc. Combust. Inst. 36 (2017) 1165-1173.

[28] H. Zhao, J. Fu, F.M. Haas, Y. Ju, Effect of prompt dissociation of formyl radical on 1, 3, 5-trioxane and CH_2O laminar flame speeds with CO_2 dilution at elevated pressure, Combust. Flame., 183, 253-260

[29] H Zhao, J Fu, Y Ju, Effect of "prompt" dissociation of formyl radical on high temperature oxidation of formaldehyde in the study of 1, 3, 5-trioxane pressurized laminar flame speeds, 55th AIAA Aerospace Sciences Meeting, 1964

[30] E. J. Zhang, B. Brumfield, and G. Wysocki, "Hybrid Faraday rotation spectrometer for sub-ppm detection of atmospheric O_2," Opt. Expr. 22, 15957-15968 (2014).

[31] Y. Wang, M. Nikodem, E. Zhang, F. Cikach, J. Barnes, S. Comhair, R. Dweik, C. Kao, and G. Wysocki, "Shot-noise Limited Faraday Rotation Spectroscopy for Detection of Nitric Oxide Isotopes in Breath, Urine, and Blood," Scientific Reports 5 (2015).

[32] B. Brumfield, and G. Wysocki, "Faraday rotation spectroscopy based on permanent magnets for sensitive detection of oxygen at atmospheric conditions," Opt. Expr. 20, 29727-29742 (2012).

[33] S.W. Benson, F.R. Cruickshank, D.M. Golden, et al., Additivity rules for the estimation of thermochemical properties, Chem. Rev. 69 (1969) 279-324.

[34] A.M. Dean, J.W. Bozzelli, Combustion chemistry of nitrogen. In: Gardiner W.C. (eds) Gas-Phase Combustion Chemistry. Springer, New York, NY (2000).

[35] <http://www.reactiondesign.com/products/chemkin/chemkin-pro/>

[36] S.S. Merchant C.F. Goldsmith, A.G. Vandeputte, et al., Understanding low-temperature first-stage ignition delay: Propane, Combust. Flame, 162, (2015) 3658-3673

Supplementary document

Experimental and Modeling Study of The Mutual Oxidation of N-pentane and Nitrogen Dioxide at Low and High Temperatures in a Jet Stirred Reactor

Hao Zhao*[1], Alon Grinberg Dana[2], Zunhua Zhang[3], William H. Green[2], Yiguang Ju[1]

[1]Department of Mechanical and Aerospace Engineering,

Princeton University, Princeton, NJ 08544-5263, USA

[2]Department of Chemical Engineering,

Massachusetts Institute of Technology, Cambridge, MA, 02139-4307, USA

[3]School of Energy and Power Engineering,,

Wuhan University of Technology, Wuhan 430063, China

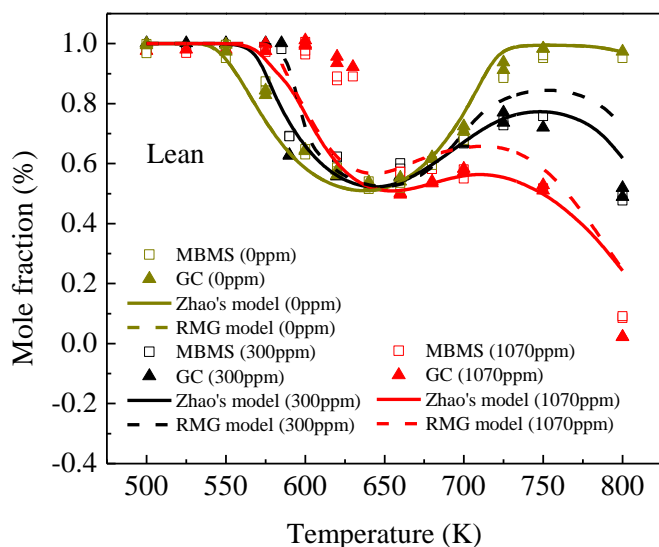*[*]Corresponding Author Email: haozhao@princeton.edu*

Fig. S1 Temperature evolution of the mole fraction of n-pentane in the oxidation mixtures of 1% n-pentane/16% O_2/5% Ar/78% N_2/0ppm NO and 1% n-pentane/16% O_2/4.89% Ar/78% N_2/1070ppm NO at 500-800K in an atmospheric-pressure JSR.

Table S1 Modified rate coefficients of $RO_2 + NO$, $NO_2 + CH_3$, $NO_2 + HO_2$, $NO + OH$, and $NO + HO_2$[a]

Reaction	A (cm^3, mol, s)	n	Ea (cal/mol)	A factor modification	comments
$C_5H_{11}O_2$-1 + NO = $C_5H_{11}O$-1 + NO_2	6.325E+13	0	1058	-	b
$C_5H_{11}O_2$-2 + NO = $C_5H_{11}O$-2 + NO_2	6.325E+13	0	1058	-	b
$C_5H_{11}O_2$-3 + NO = $C_5H_{11}O$-3 + NO_2	6.325E+13	0	1058	-	b
$NO_2 + CH_3 = NO + CH_3O$	1.400E+14	0	0	x10	c
$NO_2 + HO_2 = HONO + O_2$	1.446E+10	0	0	x0.2	d
$NO + HO_2 = NO_2 + OH$	5.00e+12	0	-477	x2.27	e
$NO + OH + M = HONO + M$	5.97E+12	-0.05	-721.00	x3	f
	Low/1.524E+24	-2.51	-67.60	x3	

[a] For the modified Arrhenius form $k = A \cdot T^n \cdot e^{Ea/RT}$

[b] Taken from Zhao's n-pentane/NOx model, reference [13] in this study. Analogy of CH_3O_2 + NO = CH_3O + NO_2 from R. Atkinson, D.L. Baulch, et al., J. Phys. Chem. Ref. Data, 26 (1997) 521 [c] Taken from N.K. Srinivasan, et al J. Phys. Chem. A, 109 (2005) 1857-1863

[d] taken from K. Zhang et al., Proc. Combust. Inst. 34 (2013), 617-624

[e] Taken from A.M. Dean, J.W. Bozzelli (2000) Combustion Chemistry of Nitrogen. In: Gardiner W.C. (eds) Gas-Phase Combustion Chemistry. Springer, New York, NY

[f] Taken from Mueller et al., Int. J. Chem. Kin. 31 (1999) 705-724